



Structure Determination of Al₂CuMg Precipitates in AlCu₁₅Mg₅ Alloys by High-Resolution Electron Microscopy

Biljana Zlaticanin*

University of Montenegro, Faculty of Metallurgy and Technology, 810 00 Podgorica, Montenegro

Received: 14 April 2021; Accepted: 21 September 2022

In this paper, the structure of the S - phase (Al₂CuMg) precipitate in Al matrix in high-copper AlCu₁₅Mg₅ alloys has been determined by using a high-resolution electron microscopy. Al₂CuMg precipitate improve the mechanical properties of the AlCu₁₅Mg₅ alloy because the precipitates act to impede dislocation motion through the material. The two alloys AlCu₁₅Mg₅, without of Ti and with 0.3%Ti, reveal a similar density of precipitate with a particle size ranging from 50nm up to 80nm in length. The precipitates have an irregular shape and precipitates in the [2 1 4] direction. The precipitates mainly composed of Al, Cu and Mg and homogeneously distributed throughout the matrix. Small-size particles and dislocations observed by TEM with EDS mapping showing the copper rich nature of particles. Al, Cu, Mg were detected by EDS, and EDS maps suggests that they correspond to Al₂CuMg.

Keywords: Al alloys, Al₂CuMg precipitate, Hardness, High-resolution electron microscopy, Precipitation sequence

1 Introduction

Excellent strength vs. density ratio, formability and corrosion resistance, make AlCuMg alloys a potential candidate for a number of industrial applications¹. Their mechanical properties² are based on a dispersion of S – phase precipitates, which have the composition Al₂CuMg. The crystal structure of S - phase has been studied using different diffraction techniques for more than seven decades. Several models have been proposed for the structure of S-phase¹. The first model was given by Perlitz and Westgren (PW) based on X-ray diffraction³. The structure is orthorhombic with unit-cell dimensions: $a=0.4$ nm, $b=0.923$ nm, and $c=0.714$ nm, space group¹ Cmcm, containing 16 atoms in the ratio Al:Cu:Mg= 2:1:1. Laves and Witte⁴ suggested that the phase extends toward Al₅Cu₂Mg₂, implying that equal amounts of the Cu and Mg atoms in Al₂CuMg are replaced by Al. Alternatively, Nishimura⁵ proposed a homogeneous S phase of composition Al₁₃Cu₇Mg₈, implying some degree of Mg substitution for Al. Mondolfo⁶ suggested a modified PW model with slightly different lattice parameters ($a=0.4$ nm, $b= 0.925$ nm, and $c=0.718$ nm). Cuisiat et al.⁷ offered a model with a unit-cell dimensions identical to Mondolfo's, but with space group Im2m containing only 8 instead of 16 atoms. Yan *et al.*⁸ proposed an orthorhombic structure with space group Pmm2, lattice parameters $a=0.4$ nm, $b= 0.461$ nm, and

$c=0.718$ nm and four atoms per unit cell in the ratio Al:Cu:Mg=2:1:1. According to the models of Cuisiat⁷ and Yan⁸ the density of the S-phase is only half that of the aluminium matrix. However, X-ray diffraction experiments performed on alloys by Perez et al.⁹ support the models of PW and Mondolfo. The heterogeneous microstructure that consists of hardening precipitates is the main strengthening source of the AlCuMg alloys¹⁰. The S-phase is one of the key strengthening precipitate phases in AlCuMg alloys¹¹. The more common Al 2024 alloy which has a higher amount of Mg (1.5% wt) shows a much greater presence of S phase precipitates and little or no θ phase precipitates¹². Our previous investigation tried to prove that alloys with higher content of copper (approximately 15mass%) have tendency to nondendritic solidification¹. We have found it very interesting from both theoretical and practical point of view (semi-solid processing) and new alloys based on that metallic system are now being considered and developed¹.

2 Materials and Methods

Experimental work can be divided in two phases¹. The first phase comprises melting and casting of high copper AlCu₁₅Mg₅ alloys¹. The designed compositions ingots were synthesized by high-purity Al (99.5%), pure Cu and pure Mg. The chemical composition (in wt. %) of the new AlCuMg alloy was specified by quantometry analysis and the results are reported in

*Corresponding author (E-mail: biljana@vge.ac.me)

Table 1 — Chemical composition of the investigated alloys (in mass%)

TYPE OF SAMPLE	%Fe	%Si	%Ti	%Cu	%Zn	%Mg	%V	%Cr	%Mn
AlCu15Mg5 (0%Ti)	0.20	0.10	0.003	15.31	0.08	5.897	0.004	0.005	0.014
AlCu15Mg5 (0.3%Ti)	0.21	0.11	0.342	15.44	0.08	5.645	0.011	0.005	0.015

Table 1. AlCuMg alloy with chemical composition being Cu:15%, Mg:5%, Al: balance (mass percentage), was used in present experiment. The cast structure was modified by the addition of the AlTi5B1 to give alloys containing 0 to 0.3 mass.% titanium. Cast samples aged at room temperature for three months. With ageing at room temperature (natural ageing), the mechanical properties could be stable after some days, especially for 2000 series¹³. The second phase includes characterization of cast samples by X-ray powder diffraction method, SEM, TEM, EDS, DSC. Examination with scanning electron microscope (SEM) was carried out to analyze precipitates and grain structure at the higher resolution. The nanostructure was observed using a Transmission Electron Microscopy JEOL 2010. Chemicals elements presents in some precipitates were identified with a TEM/STEM microscope, operating at 200 kV and equipped with an energy dispersive X-ray spectroscopy (EDS system). DSC analyses have been performed in a differential scanning calorimeter type Shimadzu DSC-50 under protective argon atmosphere¹, at a scanning rate of 10°C/min, to the maximum temperature of 725°C. Mass of tested samples has been in range of 15.02-15.17 mg. This method has produced DSC - curve on the basis of which next parameters have been calculated: heat of transition. Hardness of the samples has been measured by use of the Brinell method¹. Compression strength of the samples of cast alloys has been tested on a universal electronic tensile testing machine¹ of 1x10⁴ kg. Average size of samples was as follows: diameter Do=10mm and height Ho=20mm. All of the tested samples have been fractured¹. Compression strength is measured in the moment of fracture¹.

3 Results and Discussion

The structure of S precipitate phase in AlCu₁₅Mg₅ alloys is the subject of the current paper. The structure was observed using an X-ray powder diffraction method¹, and obtained results for the lattice parameters of orthorhombic intermetallic compound² Al₂CuMg for AlCu₁₅Mg₅ alloy are: a=0.4008 nm, b=0.9246 nm, c=0.7173 nm and V = 0.2658 nm³. The determination of precipitate crystal structure by diffraction experiments can be complicated¹⁴ by several factors:

weak diffraction spots above the Al background scattering, significant overlap between precipitate and Al peaks, and low contrast between neighboring elements, such as Mg and Al¹⁴. Since Al₂CuMg precipitates in Al – based matrices have dimensions in the range of nanometers, they cannot be successfully investigated using X-ray diffraction techniques. For nanometer scale structures, electron microscopy and high – resolution imaging become indispensable tools in structure determination. From the X-ray diffractograms the following microstructural parameters calculated: the microvoltage is 0.1611 mV and the dislocation density is 12.44 x 10¹⁰ cm⁻². The X-ray examination of the AlCu15Mg5 alloys with and without addition of Ti showed very high microvoltage values, which were expected because of the way the alloys were manufactured and the method used for their investigation. Because of the supportive evidence from X-ray data, electron diffraction and previous studies of the S –phase structure, it was concluded that any proposed structure should have the stoichiometry Al:Cu:Mg of 2:1:1, lattice parameters similar to those originally reported by Perlitz and Westgren (PW). In this alloys S precipitates are usually seen to form heterogeneously on dislocations, and in other words, a higher density of dislocations plays an important role in precipitation, resulting in the strengthening of the metals. Moreover, it is easier to precipitate S –phases at the grain boundary. These precipitates impede the movement of dislocations and lead to attain higher strength and other better mechanical properties.

Figure 1 shows intermetallic particles detected with SEM. Chemicals elements presents in precipitate were identified with a TEM microscope. The EDS mapping analysis was performed and maps of the elements Cu, Al and Mg are shown in Fig. 2. By careful analysis of experimental images taken of Al₂CuMg phase in aluminium (Figs 2-5), it is seen that the precipitation processes lead to the formation of S – phase. The two alloys AlCu₁₅Mg₅, without of Ti and with 0.3%Ti, reveal a similar density of precipitate with a particle size ranging from 50nm up to 80 nm in length. The precipitates have an irregular shape and precipitates in the [2 1 4] direction. The precipitates mainly composed

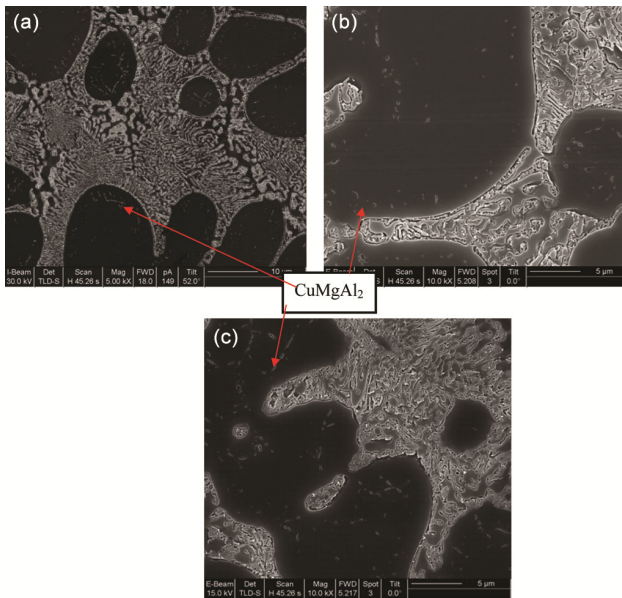


Fig. 1 — SEM micrograph of the microstructure in AlCu₁₅Mg₅ (0.3%Ti) alloy: (a), (b) and (c).

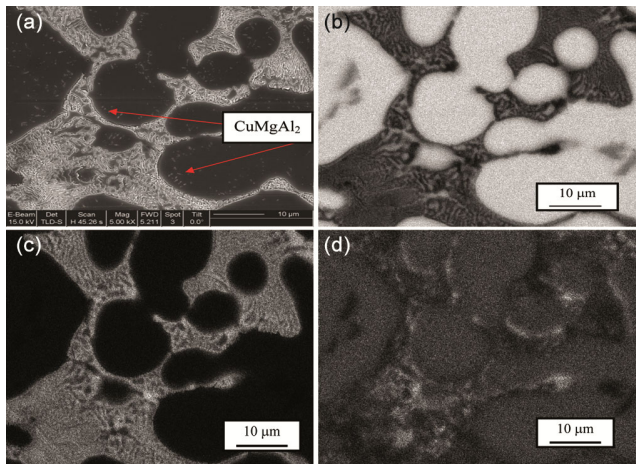


Fig. 2 — Micrograph of the microstructure in AlCu₁₅Mg₅ (0.3%Ti) alloy: (a) electron image, (b) Al distribution, (c) Cu distribution, and (d) Mg distribution.

of Al, Cu and Mg and homogeneously distributed throughout the matrix. Small-size particles and dislocations observed by TEM with EDS mapping showing the copper rich nature of particles. Composed of mainly Cu, these small size intermediate particles participate in hardening¹⁵. Al, Cu, Mg were detected by EDS, and EDS maps suggests that they correspond to Al₂CuMg. The distribution of the S-phase in Figs 2-5 shows that the S phase nucleates heterogeneously on dislocations and on grain-boundary. The precipitation of S -phase follows the pattern typical of other aluminium alloys with the initial zone and/or coherent stage

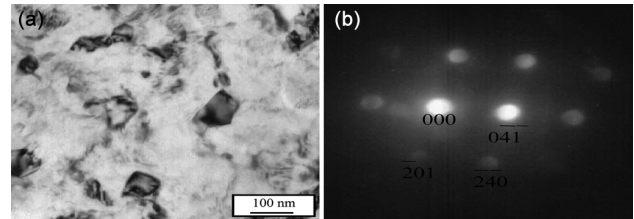


Fig. 3 — TEM micrographs and corresponding diffraction patterns of the AlCu₁₅Mg₅ (0%Ti) alloy. (a) S phase precipitate with surrounding matrix of Al, and (b) The diffractogram of the Al₂CuMg - phase obtained to the [2 1 4] matrix zone axis - selected area diffraction (SAD) pattern.

of precipitation, then precipitation of a single semi-coherent modification of the equilibrium phase and, finally, the formation of the equilibrium phase¹⁵. The precipitation sequence for AlCuMg alloys has been studied for decades. The possible precipitation sequences for AlCuMg alloys follow the following steps¹⁵:

Supersaturated solid solution (SSS) → GP zone → θ' → θ' → θ-Al₂Cu, or

Supersaturated solid solution (SSS) → GPB zone → S'' → S' → S-Al₂CuMg

with GP and GPB being Guinier-Preston and Guinier-Preston-Bagaryatsky zones respectively. θ' and S' are metastable phases forming upon artificial aging and whose presence leads to the maximum hardening state¹⁵. In the early stages of aging, coherent precipitates form [called Guinier-Preston-Bagaryastskii (GPB) zones], although the precise structure of these zones is not known¹⁴. Equilibrium precipitates (θ-Al₂Cu and S-Al₂CuMg) are larger¹⁵.

In AlCu₁₅Mg₅ alloys the precipitation sequence is: Solid solution → GPB zones → S. For the purposes of this paper, we do not distinguish between S'', S', and S, but rather consider only the equilibrium S phase. However, it is suggested that the low Cu/Mg ratio promotes the formation of the S-phase¹⁶⁻¹⁷. Dislocations are indeed pinned by these small size particles, which proves that they contribute to the hardening of the material by hindering the movement of dislocations¹⁸. The diffractogram of the S - phase (Al₂CuMg) on Fig. 3 shows a image obtained to the [2 1 4] matrix zone axis, and the diffractogram of the Al₂CuMg on Fig. 4 shows a image obtained to the [0 6 1] matrix zone axis. These type of small particles observed in both alloys. Also a lot of dislocations were observed by TEM in the both AlCu₁₅Mg₅ alloys. The latter precipitation sequence leading to S-Al₂CuMg was of controversial matter until recently¹⁹⁻²¹, particularly about the crystallographic structure of the lath shape S'' and S' phases. It is now believed that

these two phases have a crystalline structure identical to the equilibrium S phase but with varying lattice dimensions²².

The hardness of the modified AlCu₁₅Mg₅ alloy is 173 HB and is slightly higher than the hardness of the alloy without any modification treatment which is 165 HB. By increasing the content of titanium the compression strength also increase from 705 MPa for AlCu₁₅Mg₅ (0%Ti) to 712 MPa for AlCu₁₅Mg₅ (0.3%Ti). Natural ageing results in a increase in hardness, the values of 173 HB for modified AlCu₁₅Mg₅

and 165 HB for the alloy without any modification treatment are higher, respectively, than the 167 HB for AlCu₁₅Mg₅ (0.3%Ti) and 161 HB for AlCu₁₅Mg₅ (0%Ti), but close to their original state. The formation of Al₂CuMg precipitates clusters induces local stresses in their vicinity²³, thus causing an increase in the hardness of the alloy. During deformation, the dislocations motion is greatly impeded by these precipitates which results in an increase of the YS, UTS, and FS of the material²⁴.

TEM and DSC have been used to study the formation of S phase precipitation in an AlCu₁₅Mg₅ alloy. We have calculated the enthalpies of formation of the Al₂CuMg phase and the result is -8.47 kJ/mol, and this reasonable (negative) formation enthalpy is in good agreement with the measured formation enthalpy of Notin et al.²⁵ and with the measured formation enthalpy of Perlitz and Westgren³ (Table 2). Very recently, Radmilovic, Kilaas, Dahmen, and Shiflet (RKDS) have re-evaluated the structure of S phase precipitates using quantitative HREM¹⁴. The RKDS model resulting in a positive formation enthalpy and

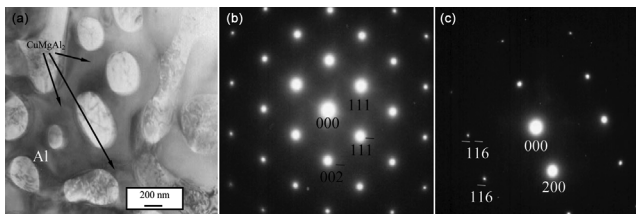


Fig. 4 — TEM micrographs and corresponding diffraction patterns of the AlCu₁₅Mg₅ (0.3%Ti) alloy: (a) S phase precipitate with surrounding matrix of Al, (b) The diffractogram of the Al₂CuMg - phase obtained to the [0 6 1] matrix zone axis

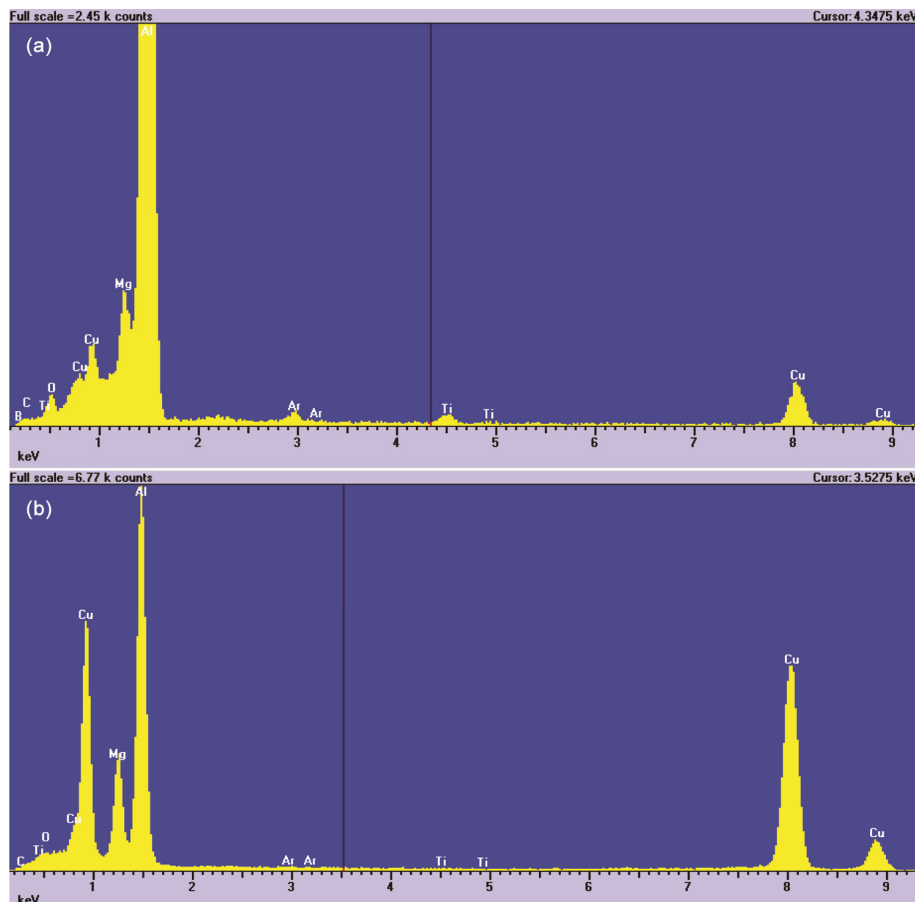


Fig. 5 — EDS microanalysis: (a) α (Al) solid solution, and (b) S phase precipitate in Al.

Table 2 — Comparison of our experimental enthalpies of formation (kJ/mol) of the Al₂CuMg phase with the measured values of Perlitz and Westgren and the measured formation enthalpy of Notin

PHASE	Experiment
CuMgAl ₂ S - experiment	-8.47
CuMgAl ₂ S (PW)	-19.4
CuMgAl ₂ S (Notin et al.)	-15.8
CuMgAl ₂ S (RKDS model)	+16.4

Table 3 — Comparison of our experimental structural parameters of S phase with the measured values of Perlitz and Westgren

Parameters	Perlitz i Westgren	Experiment
a (nm)	0.400 - 0.403	0.399 - 0.405
b (nm)	0.923 - 0.930	0.921 - 0.933
c (nm)	0.708 - 0.718	0.706 - 0.717
V (nm ³)	0.2636 - 0.2657	0.262 - 0.267

this suggests that the RKDS model for S is unstable with respect to phase separation into the constituent metals, Al, Cu, and Mg¹⁴. Table 3 gives the experimental structural parameters of the S phase, compared with the measured values of Perlitz and Westgren. The lattice constants are in reasonable agreement with experiment, and this agreement further suggests that the PW (Perlitz and Westgren) model is correct.

4 Conclusion

In this paper, a new type of AlCuMg alloy was studied. A combination of SEM, TEM and EDS mapping was carried out to reveal the composition of the precipitates in AlCu₁₅Mg₅ alloy. The major precipitates in present AlCu₁₅Mg₅ alloy are S precipitates. The calculated properties of S precipitates agree well with experiment for lattice constants and formation enthalpies. Using electron microscopy it was confirmed that the structure model proposed by Perlitz and Westgren is the only right model for well-developed S-phase precipitates. The microstructure of the alloy contains a high density of the S-phase precipitates nucleated on dislocations. For Cu/Mg ratio 3, the precipitation sequence leads to the formation of S-Al₂CuMg phase, which means that Al₂CuMg precipitates should be the principal hardening agent. In practical application, the nanometer-sized S phase precipitates are key strengthening precipitates in high-

strength AlCu₁₅Mg₅ alloys. Aging at room temperature of the AlCu₁₅Mg₅ alloys leads to an increase of hardness in all studied alloys.

References

- Zlaticanin B, Radonjic B, & Filipovic M, *Mater Trans*, 45 (2004) 440.
- Kilasa R, & Radmilovic V, *Microscopy and Microanalysis*, 6 (2020) 1030.
- Perlitz H, & Westgren A, *Ark. Kemi Mineral Geol*, 16B (1943) 1.
- Laves F, & Witte H, *Metallwirtschaft*, 15 (1936) 15.
- Nishimura H, *Mem. Colloid Eng. Kyoto Imp. Univ*, 10 (1937) 18.
- Mondolfo L F, *Aluminium Alloys: Structure and Properties*, (Butterworth - Heinemann, London), 1st Edition, eBook ISBN: 9781483144825, 1976, p. 497.
- Cuisiat F, Duval P, & Graf R, *Scr Metall*, 18 (1984) 1051.
- Yan J, Chunzhi L, & Minggao Y, *J Mater Sci Lett*, 9 (1990) 421.
- Perez-Landazabal J I, Madariaga G, & Juan J S, *J Mater Res*, 12 (1997) 577.
- Cheng S, Zhao Y H, Zhu Y T, & Ma E, *Acta Mater*, 55 (2007) 5822.
- Liu Z R, Chen J H, Wang S B, Yuan D W, Yin M J, & Wu C L, *Acta Materialia*, 59 (2011) 7396.
- DeRose J A, Bałkowiec A, Michalski J, Suter T, Kurzydłowski K J, & Schmutz P, *Transactions on State of the Art in Science and Engineering*, 61 (2012) 23.
- Tafti M F, Sedighi M, & Hashemi R, *Iranian Journal of Materials Science & Engineering*, 15 (2018) 1.
- Wolverton C, *Acta mater*, 49 (2001) 3129.
- Cochard A, Zhu K, Joulié S, Douin J, & Huez J, *Materials Science and Engineering: A*, 690 (2017) 259.
- García-Hernández J L, Garay-Reyes C G, Gómez-Barraza I K, Ruiz-Esparza-Rodríguez M A, Gutiérrez-Castañeda E J, Estrada-Guel I, Maldonado-Orozco M C, & Martínez-Sánchez R, *J Mater Res Technol*, 8 (2019) 5471.
- Wang S C, & Starink M J, *Int Mater Rev*, 50 (2005) 193.
- Tolley A, Ferragut R, & Somoza A, *Philosophical magazine*, 89 (2009) 1095.
- Moy C K S, Weiss M, Xia J, Sha G, Ringer S P, & Ranzi G, *Materials Science and Engineering: A*, 552 (2012) 48.
- Wang S C, & Starink M J, *Acta Materialia*, 55 (2007) 933.
- Styles M J, Hutchinson C R, Chen Y, Deschamps A, & Bastow T J, *Acta Materialia*, 60 (2012) 6940.
- Sha G, Marceau R K W, Gao X, Muddle B C, & Ringer S P, *Acta Materialia*, 59 (2011) 1659.
- Gurugubelli S N, *World Acad Sci Eng Technol*, 62(2012) 648.
- Afzal N, Shah T, & Ahmad R, *Problemi Procnosti*, 6 (2013) 69.
- Notin M, Dirand M, Bouaziz D, & Hertz J, *CR Acad Sci Paris*, 302 (1986) 63.